ELSEVIER

Thermochimica Acta 348 (2000) 115–120

thermochimica acta

www.elsevier.com/locate/tca

Thermal properties and devitrification behavior of $(2.5-x)CaO{\cdot}x/3La_2O_3{\cdot}2SiO_2$

A. Costantini*, G. Luciani, F. Branda

Dipartimento di Ingegneria dei Materiali e della Produzione, Università di Napoli, Napoli, Italy

Received 14 July 1999; received in revised form 9 December 1999; accepted 14 December 1999

Abstract

La_2O_3 was substituted for CaO in a glass of composition $2.5CaO{\cdot}2SiO_2$ and the effect of this substitution on thermal properties and non-isothermal behavior was studied. The glass samples were submitted to thermal analysis (DTA) and X-ray diffraction analysis. The trends with the composition of the glass transformation, T_g, and the activation energy of crystal growth, E_c, are the result of a type of competition between Ca^{2+} and La^{3+} ions each to achieve their preferred coordination. The lanthanum ion does not succeed in realizing its own average coordination. As a result $T_g=810\pm5$°C and the activation energy for crystal growth was $E_c=650\pm25$ kJ/mol, regardless of composition. Devitrification involved a mechanism of surface nucleation: however, because the samples softened and sintered before devitrifying, surface nuclei behaved as bulk nuclei. In all the devitrified samples $CaO{\cdot}SiO_2$ crystals form together with a secondary calcium silicate phase, while $Ca_3La_6(SiO_4)_6$ crystals form when ≅40% molar weight CaO is substituted. The pattern for the La_2O_3 free glass shows that the $\alpha CaO{\cdot}SiO_2$ is also formed in the temperature range 900–1000°C, which should be stable only above 1125°C as reported in the phase diagram.

Keywords: Activation energies; Crystal growth; Calcium lanthanum silicate; Non-isothermal devitrification

1. Introduction

It is known that glasses of the system $CaO\text{-}SiO_2$ with a CaO molar fraction in the range 0.3–0.55 are bioactive, that is to say they bond to living bone through a thin layer rich in calcium and phosphorus [1,2]. The addition of La_2O_3 to silicates improves both elastic modulus and hardness of the glasses [3]. Recently, it was found [4,5] that the non-isothermal devitrification of glasses of composition $CaO\text{-}La_2O_3(MgO)\text{-}SiO_2$ exhibited peculiar characteristics. These devitrify through a surface nucleation mechanism. However, since in the temperature range of efficient crystal growth, softening and sintering occur, surface nuclei behave virtually as bulk nuclei. This was well supported by SEM observations for samples devitrified during a DSC run [6].

In this paper the thermal properties and the study of the devitrification behavior of glasses of composition $(2.5-x)CaO{\cdot}x/3La_2O_3{\cdot}2SiO_2$ are reported. The substitution kept the O/Si molar ratio constant.

2. Experimental

Glasses of composition expressed by the following formula

$$(2.5-x)CaO\cdot x/3La_2O_3\cdot 2SiO_2$$

were prepared by melting analytical grade reagents, La_2O_3, $CaCO_3$ and SiO_2 in a platinum crucible in an

* Corresponding author. Tel.: +39-81-7682400; fax: +39-81-7682404.
E-mail address: anicosta@unina.it (A. Costantini)

0040-6031/00/$ – see front matter
PII: S0040-6031(00)00364-6

electric furnace for 4 h, in the temperature range 1400–1600°C. The melts were quenched by plunging the bottom of the crucible into cold water. The products were weighted after quenching and it was found that losses were not greater than 0.5%.

Differential thermal analysis (DTA) was carried out by means of a Netzsch differential scanning calorimeter (DSC) model 404M on approximately 50 mg powdered samples at various heating rates (2–20°C/min). Finely (63–90 μm) and coarsely (315–500 μm) powdered samples were used. Powdered Al_2O_3 was used as reference material. In order to calibrate the instrument, a preliminary DTA was carried out using Al_2O_3. The DTA curve obtained did not show any inflection in the baseline.

Devitrified samples were analyzed by computer-interfaced X-Ray (Cu Kα) powder diffractometry (XRD) using a Philips Diffractometer model PW1710, with a scan speed of 1°/min and a built-in computer search program. The crystalline phases were identified by means of JCPDS cards.

3. Results

Figs. 1 and 2 show the DTA curves obtained for finely and coarsely powdered samples, respectively. As illustrated in Fig. 3, the glass transformation temperature, T_g, was taken as the maximum of the DDTA curve in the glass transformation range. In the same figure, the DTA exothermic peak temperature T_p is also shown. The uncertainty of both values is of approximately ±1°C. In Fig. 4 T_g and T_p values are plotted against the glass composition expressed as the x values of the general formula of the series. The substitution appears to have no effect on T_g, while a slight increasing trend was observed for T_p.

Fig. 5 shows the X-ray diffraction patterns of the samples submitted to a DTA run stopped just after the exothermic peak. The lines were attributed by means of the JCPDS cards. In all patterns, the lines of wollastonite (JCPDS card 27/88) appear. In the (a) pattern (x=0), the lines of pseudo-wollastonite, $\alpha CaO{\cdot}SiO_2$ (JCPDS card 19/248) and $3CaO{\cdot}SiO_2$ (JCPDS card 11-593) are also present. It is interesting

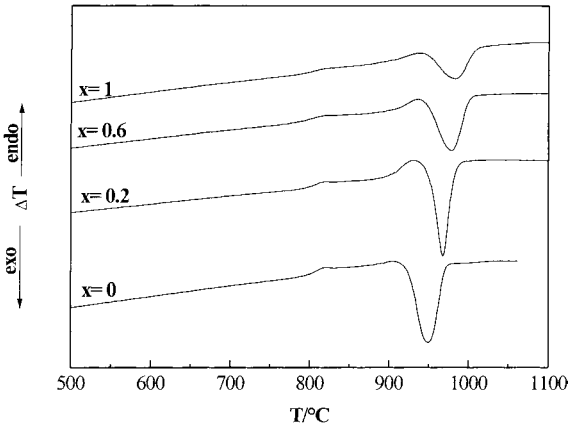

Fig. 2. DTA curves recorded at 10°C/min on coarsely (315–500 μm) powdered samples.

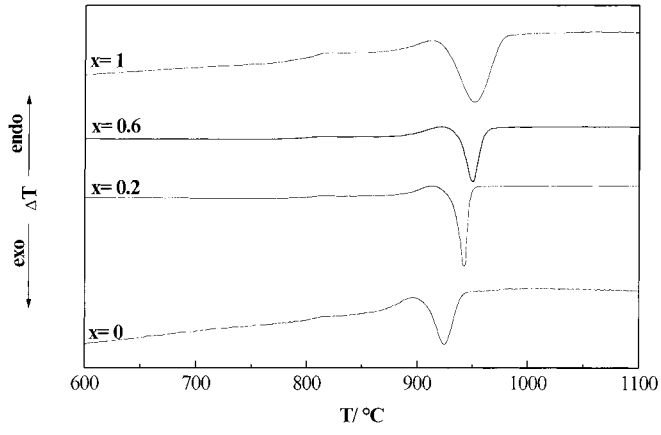

Fig. 1. DTA curves recorded at 10°C/min on finely (63–90 μm) powdered samples.

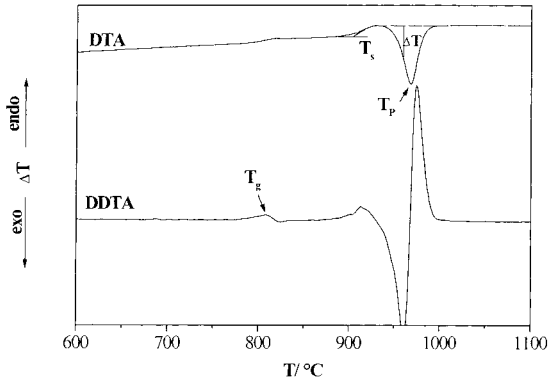

Fig. 3. A typical DTA curve and its first derivative (DDTA).

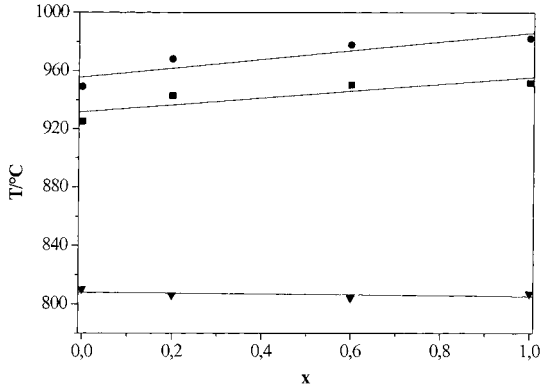

Fig. 4. Glass transformation temperature, T_g (▼) and peak temperature T_p for finely (■) and coarsely powdered (●) samples vs. composition (x).

to observe that $\alpha CaO{\cdot}SiO_2$ is the high temperature phase, in fact in the phase diagram $CaO{\cdot}SiO_2$ is reported to be stable above 1125°C. In the ((b), (c) and (d)) patterns, they are partially substituted by the lines of $2CaO{\cdot}SiO_2$ (JCPDS card 24-234); in the (c) and (d) patterns (x=0.6, 1.0) $Ca_3La_6(SiO_4)_6$ crystal (JCPDS card 27/78) reflections appear.

Non-isothermal devitrification was also studied. The kinetic parameters were determined using the following two equations:

$$\ln\beta = -\frac{E_c}{RT_p} + \text{const} \quad (1)$$

$$\ln\Delta T = -\frac{mE_c}{RT} + \text{const} \quad (2)$$

that can be derived from the well-known following expression [7,8]:

$$-\ln(1-\alpha) = \left(\frac{AN}{\beta^m}\right)\exp\left(-\frac{mE_c}{RT}\right) \quad (3)$$

where α is the crystallization degree, N is the nuclei number, A is a constant, β is the heating rate, ΔT and T_p are, respectively, the deflection from the baseline and the peak temperature taken as indicated in Fig. 3.

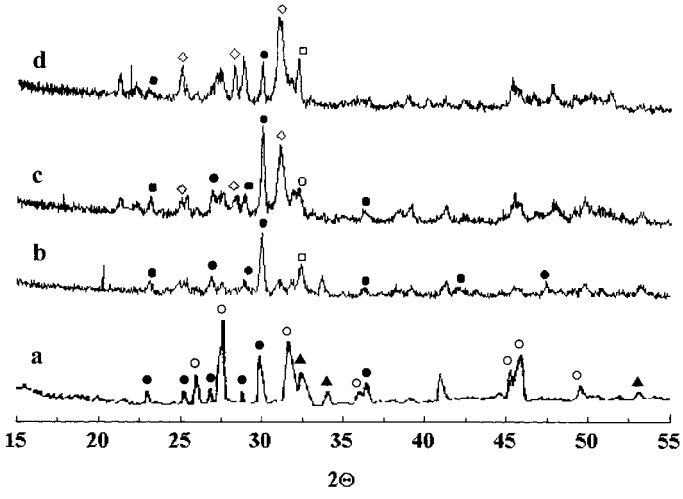

Fig. 5. X-ray diffraction patterns of samples devitrified during a DTA run: (●) wollastonite; (○) pseudo-wollastonite; (■) $3CaOSiO_2$; (□) $2CaOSiO_2$; (◇) Ca_3La_6 $(SiO_4)_6$.

Since in silicate glasses the devitrification exo-peak occurs in a higher temperature range than that of efficient nucleation [4], E_c is the crystal growth activation energy. The parameter m depends on the mechanism and morphology of crystal growth; it ranges from m=1 for one-dimensional growth to m=3 for three-dimesional growth [7,8].

Eqs. (1) and (2) can be derived from Eq. (3) by supposing that: (1) the value of α at peak temperature is not dependent on the heating rate [9]; (2) ΔT is proportional to the instantaneous reaction rate [10,11]; (3) in the initial part of the DTA crystallization peak the deflection from the baseline, ΔT, is assumed to be constant with the crystallization degree, α, since the change in the temperature has a much greater effect on it [12]. Eq. (1) was obtained using Kissinger method. It was compared to Ozawa method [13,14] and it was shown that, since the changes of β are dominant with respect to $T_{\alpha 0}^{2n}$, equation

$$\frac{1}{n}\ln\left(\frac{\beta^{n+1}}{T_{\alpha 0}^{2n}}\right) = c2 - \frac{E}{R}\frac{1}{T_{\alpha 0}} \tag{4}$$

can be reduced to

$$\frac{1}{n}\ln\beta^{n+1} = c2 - \frac{E}{R}\frac{1}{T_{\alpha 0}} \tag{5}$$

In Fig. 6 the plots of ln β versus $1/T_p$ are reported. In Figs. 7 and 8 the plots of ln ΔT versus $1/T$ are reported for finely and coarsely powdered samples. According to Eqs. (1) and (2) straight lines were obtained. Their slopes allow the determination of values of E_c and mE_c

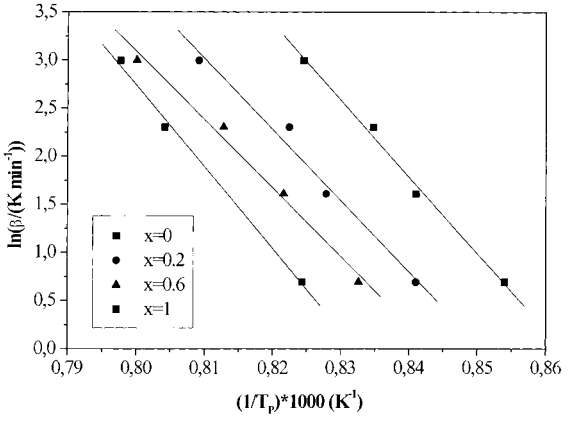

Fig. 6. Kissinger plot of ln β vs. $1/T_p$.

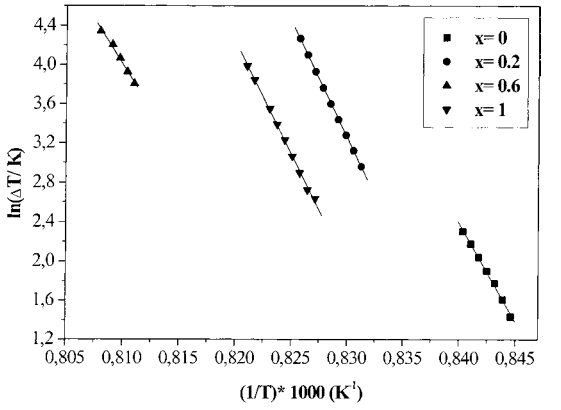

Fig. 7. ln ΔT vs. $1/T$ for finely powdered (63–90 μm) samples.

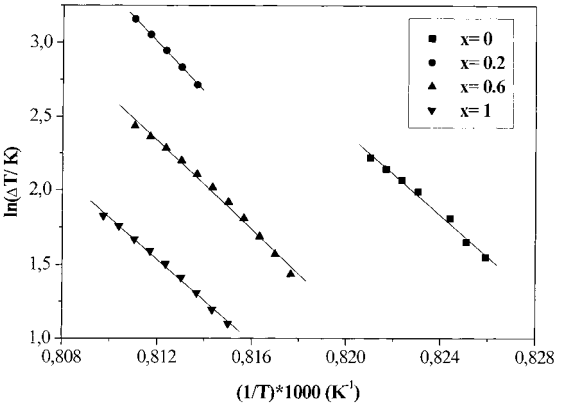

Fig. 8. ln ΔT vs. $1/T$ for coarsely powdered (315–500 μm) samples.

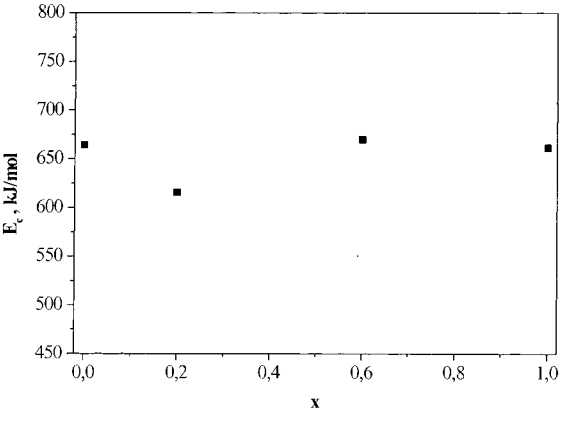

Fig. 9. Activation energy of crystal growth, E_c vs. composition (x).

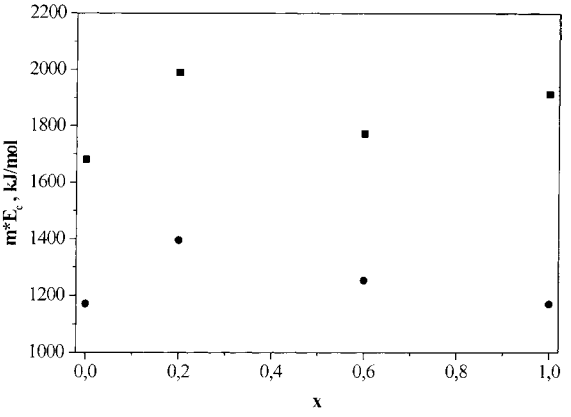

Fig. 10. mE_c values for finely (63–90 μm) (●) and coarsely powdered (315–500 μm) (■) samples vs. composition (x).

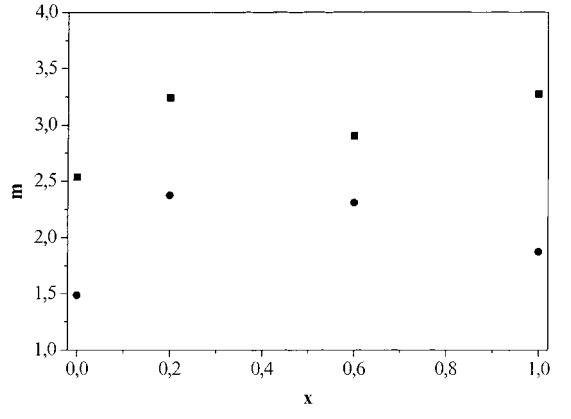

Fig. 11. m values for finely (63–90 μm) (■) and coarsely powdered (315–500 μm) (●) samples vs. composition (x).

with an error of ±10% [14] and, therefore, the magnitudes of m for each glass. In Figs. 9–11, E_c, mE_c and m values, respectively, are reported as a function of the composition. Only slight variations of E_c values are obtained as x increases. It is interesting to observe that the m values relative to finely powdered samples are greater than the ones relative to coarsely powdered samples.

4. Discussion

The role of SiO_2 and CaO in the glass structure is well known: the former is a network former oxide, while the latter in a network modifier. La_2O_3 is a less common component of glasses. The criterion reported in the literature [18,20] suggest that it is expected to be a network modifier. This role proved to be useful in explaining T_g versus composition curves of glasses of the system Na_2O-M_2O_3-SiO_2 (M=La, Sc, Y, Al, B) obtained by substituting M_2O_3 for Na_2O starting from the glass composition $Na_2O{\cdot}2SiO_2$ [19].

Following Ray [17], T_g values depend on the density of covalent cross-linking and the numbers and strengths of cross-linking between the oxygens and the cations. In the series studied the ratio O/Si is constant, therefore no change in the covalent cross-linking density occurs. Hence, in this case, any differences in T_g value must be attributed to changes of the numbers and strengths of cross-linking of the network modifier cations, having their own coordination and field strength, Z/r^2 (where Z is the charge and r the radius of the cation) [18,20]. Here, Ca^{2+} and La^{3+} have closely similar field strength values, $Z/r^2 = 2.04\ Å^{-2}$, while small differences in the average coordination number in the glass can be expected as a consequence of the greater radius of the La^{3+} ion (1.21 Å instead of 0.99 Å). Fig. 4 shows no variations of T_g as La_2O_3 substitutes CaO. This trend of T_g curve is also consistent with previous results [4,15]: when the cations have similar Z/r^2 values, changes due to different coordination number occur when the amount substituted is sufficiently great. This was interpreted as the result of some competition between the two cations to achieve their preferred coordination. Therefore, the experimental results suggest that in the quenched glasses the lanthanum ion does not succeed in realizing its own average coordination. Whereas T_g depends on the structure of the glasses, T_p depends on the kinetic parameters of the devitrification process.

When considering the activation energy for crystal growth it is worth remembering that E_c is usually equal to the viscous flow activation energy E_η [16]. Because the structure rigidity does not vary and T_p shows little changes with the substitution, E_η and therefore E_c are expected to be constant; this is confirmed by our experimental results.

The m values appear to increase as the specific surface is increased (Fig. 11). Usually [21] the opposite result is obtained owing to the fact that the greater the specific surface the greater the tendency to devitrify by growth from surface nuclei so that m should be

progressively reduced to $m=1$. In the case of diopside glass [22] and glasses of composition $CaO{\cdot}SiO_2$, $1.6CaO{\cdot}0.4MgO{\cdot}2SiO_2$ and $1.4CaO{\cdot}(0.6/3)Y_2O_3{\cdot}2SiO_2$, it was found that nucleation preferentially occurs at the surfaces of the sample, but surface nuclei, formed in the glass transformation range, behave as bulk nuclei in finely powdered samples that efficiently sinter before devitrifying. This hypothesis appears to be effective in explaining the devitrification behavior of the studied glasses. In fact, in the case of coarsely powdered samples, that badly sinter, lower m values were obtained.

The evolution of XRD patterns shown in Fig. 5 is easily explained. The formation of a calcium poorer secondary phase, when CaO is substituted with La_2O_3 ($2CaO{\cdot}SiO_2$ instead of $3CaO{\cdot}SiO_2$), can be attributed to the progressive reduction of the amount of calcium available. In the devitrified glass richest in La_2O_3, the majority phase is attributed to $Ca_3La_6(SiO_4)_6$ crystals. The growth of the $\alpha CaO{\cdot}SiO_2$ phase at lower temperatures than those shown in the phase diagram is easily explained considering that a sample subjected to a non-isothermal treatment, does not necessarily approaches equilibrium. Therefore, the $\alpha CaO{\cdot}SiO_2$ phase forms at lower temperature as its growth rate is high.

5. Conclusions

The glass transformation temperature, T_g, plots suggest that the substitution of La_2O_3 to CaO caused no variations of structure rigidity. In all devitrified samples, the lines of wollastonite (JCPDS card 27-88) and of a secondary calcium silicate phase appear. The XRD pattern of the free La_2O_3 sample also shows the lines of pseudo-wollastonite (JCPDS card 19/248) which in the $CaO–SiO_2$ phase diagram is reported to be stable only above 1125°C. It is relevant that, on the contrary, the devitrified product was obtained in the temperature range 900–1000°C. In the $x=0.6$ and $x=1.0$ devitrified samples, another crystalline phase is formed whose reflections were attributed to $Ca_3La_6(SiO_4)_6$ crystals (JCPDS card 27/78). The activation energy for crystal growth E_c was 640 ± 25.1 kJ/mol regardless of composition. Devitrification involves a mechanism of surface nucleation, but, owing to softening and sintering, surface nuclei behave as bulk nuclei.

References

[1] L.L. Hench, J. Am. Cer. Soc. 74 (7) (1991) 1487–1510.
[2] T. Kokubo, Proc. XVII International Congress on Glass, Madrid Vol. 1, Bol. Soc. Esp. Ceram. Vid., 31+C1, 1992, pp. 119–137.
[3] A. Makishima, Y. Tamura, T. Sakaino, J. Am. Cer. Soc. 61 (5/6) (1978) 247.
[4] A. Costantini, R. Fresa, A. Buri, F. Branda, Silicate Industriels 7/8 (1996) 171–175.
[5] A. Costantini, F. Branda, A. Buri, J. Mat. Science 30 (1995) 1561–1564.
[6] F. Branda, A. Costantini, A. Buri, A. Tomasi, J. Therm. Analysis 41 (1994) 1479–1487.
[7] K. Matusita, S. Sakka, Bull. Inst. Chem. Res. Kyoto Univ. 59 (1981) 159–171.
[8] D.R. MacFarlane, M. Matecki, M. Poulanin, J. Non.-Cryst. Solids 64 (1984) 351–362.
[9] P.G. Boswell, J. Am. Cer. Soc. 72 (12) (1992) 3315.
[10] H.J. Borchardt, F. Daniels, J. Am. Chem. Soc. 79 (1957) 41–46.
[11] K. Akita, M. Kase, J. Phys. Chem. 72 (1968) 903–913.
[12] F.O. Piloyan, I.V. Ryabchica, O.S. Novikova, Nature 212 (2966) 1229.
[13] T. Kemeny, J. Sestak, Hungarian Academy of Sciences, Central Research Institute for Physics.
[14] J. Sestak, Phys. Chem. Glass 15 (6) (1974) 137–140.
[15] F. Branda, A. Buri, D. Caferra, A. Marotta, J. Non-Cryst. Solids 54 (1983) 193–198.
[16] K. Matusita, S. Sakka, J. Non-Cryst. Solids 38/39 (1980) 741–746.
[17] N.H. Ray, J. Non-Cryst. Solids 15 (1974) 423–434.
[18] H. Rawson, Inorganic glass forming systems, Academic Press, London and New York, 1967, pp. 24–25.
[19] A. Buri, D. Caferra, F. Branda, A. Marotta, Phys. Chem. Glasses 23 (1) (1982) 37–40.
[20] H. Scholze (Ed.), Le Verre, Institut du Verre, Paris, 1980, p. 69.
[21] A. Marotta, A. Buri, F. Branda, Thermochim. Acta 40 (1980) 397–404.
[22] F. Branda, A. Costantini, A. Buri, Thermochim. Acta 217 (1993) 207–212.